Optimal Cross-Range Pattern Synthesis Using Multi-Objective Genetic Algorithm for a Passive Antenna in Small Satellite SAR

Vinay Ravindra
Department of Electrical Engineering and Information Systems
University of Tokyo
Tokyo, Japan
Email: ravindra@ac.jaxa.jp

Hirobumi Saito and Prilando Akbar
Institute of Space and Astronautical Science/ Japan Aerospace Exploration Agency
Sagamihara, Japan
Email: koubun@isas.jaxa.jp, prilando.rakbar@jaxa.jp

Miao Zhang and Jiro Hirokawa
Tokyo Institute of Technology
Tokyo, Japan
Electrical and Electronic Engineering
Email: miao@antenna.ee.titech.ac.jp, jiro@antenna.ee.titech.ac.jp

***Abstract*—In synthetic aperture radar application, image artifacts due to azimuthal ambiguity, not-uniform main lobe antenna gain are common. They can be reduced to a certain extent by synthesizing the appropriate antenna pattern in cross-range direction. Our small satellite mission "microXSAR" carries an X-Band SAR instrument as payload, with a waveguide fed passive antenna. In this paper we describe the synthesis of the cross-range pattern of the SAR antenna by treating it as a multi-objective optimization problem. We use non-dominated sorting algorithm NSGA-II as the optimization algorithm. The result is a pareto-curve giving all possible non-dominated solutions.**

Keywords—linear antenna arrays, optimization, synthetic aperture radar

I. INTRODUCTION

In Synthetic Aperture Radar (SAR) imaging, a common image artifact is ghost images formed due to azimuthal ambiguities. Azimuthal ambiguities arise due to limited Pulse Repetition Frequency (PRF) which can be employed in a monostatic radar system. The PRF has a maximum limit to allow for unambiguous returns from the swath region defined in range direction. The Doppler spectrum is not strictly band limited (due to sidelobes of antenna pattern), and the desired signal band is contaminated by ambiguous signals from adjacent spectra [1].

Another concern is the "flatness" of the antenna beam main lobe over the illuminated azimuth region. The Noise-Equivalent Sigma naught (σ_{NEZ0}) [2] is a common evaluation metric for the signal quality. In an ideal scenario, the antenna gain will be uniform over the entire illuminated region and σ_{NEZ0} will depend only on the target reflectivity characteristics. Practically the antenna pattern cannot have flat gain over the main beam. As a compromise, a threshold value for antenna gain is chosen, and it is required for main lobe antenna gain to be above this threshold value over the desired illuminated region.

In [3], a feasibility study of X-band (9.65 GHz) SAR sensor onboard a small satellite (100 kg) is studied. A passive antenna system is favorable to allow for low complexity, low cost design and thin panels. This paper describes the synthesis of optimal cross-range pattern of a passive SAR antenna, which minimizes the above described image artifacts.

II. DESCRIPTION OF SAR ANTENNA SYSTEM

Fig. 1 shows design idea of the antenna system for the small satellite mission named as microXSAR. It consists of seven identical rectangular parallel plate aluminum panels. Each panel has array of slots which are excited in X-band and hence radiate. A rectangular waveguide feeder is used to distribute power from the satellite bus and excite the panels. "In press" [4] gives a detailed description of the antenna panel structure and measured electrical characteristics.

Fig. 2 shows a simplified model of SAR viewing geometry. η is the nadir-offset angle, H is the satellite altitude and $R(R_0, \phi)$ is the range corresponding to angle ϕ. In a spherical Earth model, maximum and minimum values of ϕ from which echoes are returned occurs when $\eta = 0$ and is given by eqn (1).

$$\phi_{hrz} = 90^0 \pm \sin^{-1} R_e/(R_e + R_0) \quad (1)$$

R_e is radius of Earth, ϕ_{hrz} is the horizon angle.

In a typical SAR mission, η varies over range of 10 deg to 45 deg. If we take the satellite in low Earth orbit, say $H = 600\ km$, we get $\phi_{hrz} \approx 24$ deg to 156 deg. The range as function of ϕ for a given η is:

$$R = R_0/\sin(\phi) \quad (2)$$

Note that eqn (2) is written assuming flat-Earth model to allow for a simplified analysis. The antenna gain pattern of the antenna is modulated by the term $1/R^2$ to account for the falling power level due to increasing range.

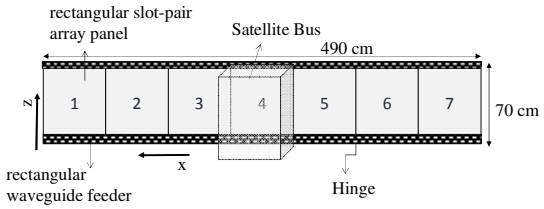

Fig.1. Antenna system of microXSAR

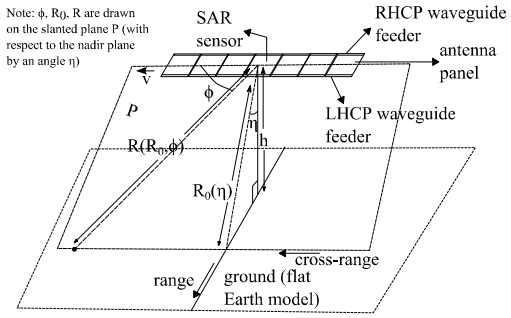

Fig. 2. SAR viewing geometry

III. Optimization

We choose a multi-objective genetic algorithm, Non-Dominated Sorting Genetic Algorithm II (NSGA-II) [5] as our optimization algorithm. The main feature of this algorithm is that it ranks the individual species according to levels of non-domination and implements elitism, storing all non-dominated solutions.

A simplified antenna model is used for optimization as shown in Fig. 3. It consists of seven point elements in a linear array, each element representing an antenna panel. Using this model we can write the field pattern $E_{cr}(\phi)$ in cross-range plane as:

$$E_{cr}(\phi) = E_{panel}(\frac{\pi}{2}, \phi) AF\left(\frac{\pi}{2}, \phi\right) \quad (3)$$

$E_{panel}(\frac{\pi}{2}, \phi)$ is the cross-range pattern of each antenna panel, also illustrated in Fig. 4.

$AF\left(\frac{\pi}{2}, \phi\right)$ is the array factor of the linear array in Fig. 3.

The image artifacts due to azimuthal ambiguity, non-uniform antenna gain over illuminated cross-range are influenced by the cross-range pattern. We define our optimization objectives as follows:

A. Maximize minimum directivity over main lobe

The far-field directivity $D\left(\frac{\pi}{2}, \phi\right)$ can be written in terms of $E_{cr}(\phi)$ as follows:

$$D\left(\frac{\pi}{2}, \phi\right) = k \left||E_{cr}(\phi)|\right|^2 / (a_0^2 + a_1^2 + \ldots\ldots + a_6^2) \quad (4)$$

k is a constant of proportionality and can be proven to be the same irrespective of the set of amplitude excitations $\{a_0, a_1, \ldots . a_6\}$ chosen.

The main lobe beamwidth is chosen to be $2\delta = \lambda/490 \text{ cm} = 0.36 \text{ deg}$.

B. Maximize modified 1-dimensional beam efficiency

To minimize azimuthal ambiguities, we must ensure returns from region other than the desired illuminated region are small. Taking into account the range modulation effect at different cross-range angles, we define a term called Modified 1-dimensional Beam Efficiency ($M.B.E.$) as follows:

$$M.B.E. = \int_{90-\delta}^{90+\delta} \left||E_{cr}(\phi)|\right|^2 \sin^2\phi \, d\phi \Big/ \int_{\phi_{hrz}^-}^{\phi_{hrz}^+} \left||E_{cr}(\phi)|\right|^2 \sin^2\phi \, d\phi \quad (5)$$

Maximizing $M.B.E$ means improved azimuthal ambiguity performance.

The optimization variables are the excitation coefficients $\{a_0, a_1, a_2, a_3, a_4, a_5, a_6\}$. Uniform phase excitation is assumed.

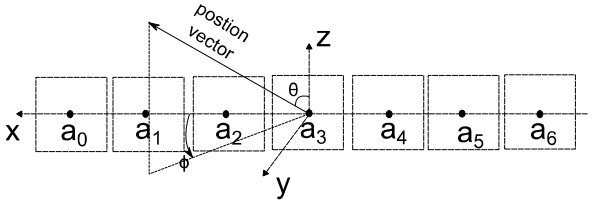

Fig.3. Linear array model of the antenna system. All the panels are similar and are approximated to single point source, uniformly spaced at distance 70cm. Cross-range pattern in formed in the XY plane.

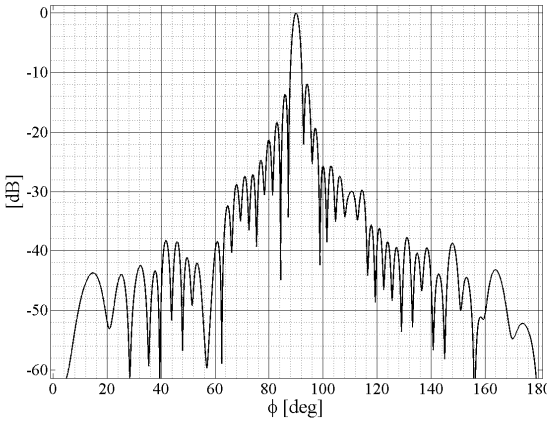

Fig. 4. Normalized antenna power pattern of single panel in XY (Cross-range) plane. See "in press" [4] for complete description.

IV. RESULTS

We run the optimization algorithm for 500 generations, 500 species, and mutation variable of value = 1/7. The pareto front converges to the concave shape as shown in Fig. 4 and remains fairly independent on use of different number of generations or different number of species.

It is useful to compare three points in the pareto graph labelled as P1, P2 and P3. P3 is a point corresponding to case of uniform excitation and is not a solution of the optimization. However it is plotted to get a better idea of the solutions. P3 is inferior in terms of the chosen objectives. P1 corresponds to the solution point which yields maximum minimum main lobe directivity, while P2 corresponds to solution point yielding maximum minimum main lobe directivity. The tradeoff between P1 and P2 is 6.8% difference in $M.B.E.$ and 0.44 dB difference in minimum main lobe directivity.

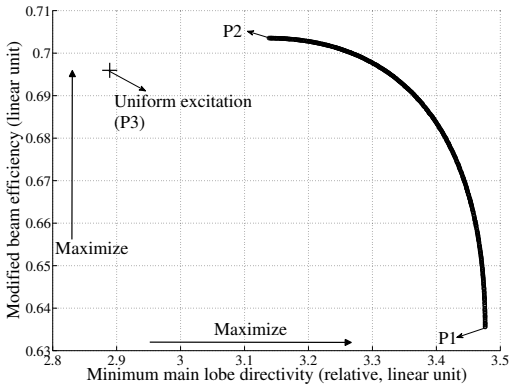

Fig. 5. Pareto Front from the optimization. The concave shape indicates that there is a tradeoff between the defined objectives.

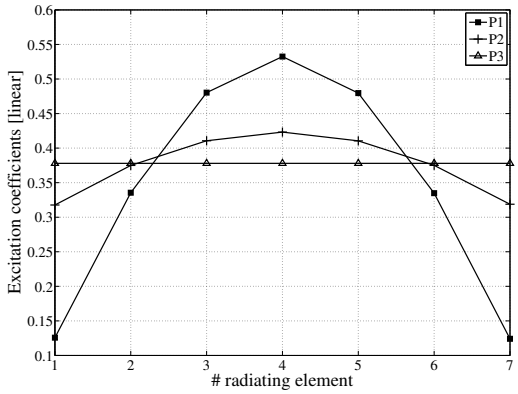

Fig. 6. Aperture excitations corresponding to points P1, P2 and P3 in the pareto graph (Fig. 5).

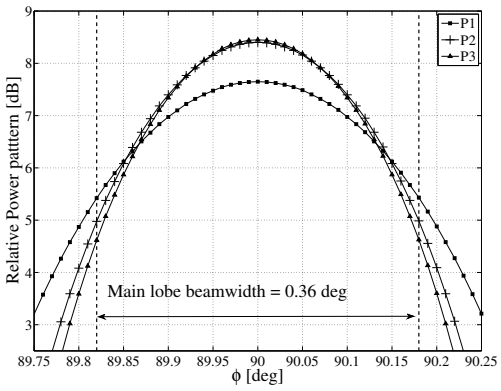

Fig. 7. Antenna main lobe field pattern corresponding to points P1, P2 and P3 in the pareto graph (Fig. 5).

V. CONCLUSION AND FUTURE WORK

Excitation synthesis of SAR cross-range pattern has been carried out using multi-objective genetic algorithm NSGA-II. The synthesized antenna pattern is optimal in minimizing azimuthal ambiguity and ensuring that the antenna gain remains above a minimum threshold level over the entire (desired) illuminated region in cross-range plane. Our future work is to realize these excitations using waveguide power divider network. A challenge in realizing this network is to ensure the excitation phase remains nearly same at all the panels over the entire frequency bandwidth of operation.

REFERENCES

[1] Curlander, R. McDonough, "System Design Considerations," in *Synthetic Aperture Radar, Systems and Signal Processing, 3*rd ed. John Wiley & Sons, Inc., 1991.

[2] M. Skolnik, "Synthetic Aperture Radar," in *RADAR Handbook, 3*rd ed. McGraw-Hill, 2008.

[3] Akbar, J. Sumantyo and H. Saito, 'Design of synthetic aperture radar onboard small satellite', in *IEICE Tech. Rep. SANE2012-80*, 2012.

[4] V. Ravindra, H. Saito, P. Akbar, M. Zhang and J. Hirokawa, "A parallel plate slot-pair array dual polarization antenna for small satellite SAR", in *International Symposium on Antennas and Propagation (ISAP2015)*, Tasmania, Australia, 2015, in press.

[5] K. Deb, A. Pratap, S. Agarwal, and T. Meyarivan, "A fast elotist multiobjective genetic algorithm : NSGA-II," in *IEEE Transactions on Evolutionary Computation*, vol. 6, no.2, April 2002, pp. 182-197.